

# Development of Biodegradable Superporous Hydrogels for Gastroretentive Delivery of Epigallocatechin Gallate

Arnas Lakhiew<sup>1</sup>, Rachanida Preparatana<sup>2</sup>, Ousanee Issarachot<sup>3</sup>, Ruedeekorn Wiwattanapatapee<sup>1,4\*</sup>

<sup>1</sup>Faculty of Pharmaceutical Sciences, Prince of Songkla University, Hat Yai, Songkhla, Thailand

<sup>2</sup>Faculty of Medical Technology, Prince of Songkla University, Hat Yai, Songkhla, Thailand

<sup>3</sup>Faculty of Public Health and Allied Health Sciences, Sirindhorn College of Public Health Trang, Trang, Thailand

<sup>4</sup>Phytomedicine and Pharmaceutical Biotechnology Excellence Center, Faculty of Pharmaceutical Sciences, Prince of Songkla University, Hat Yai, Songkhla, Thailand

Received: 29<sup>th</sup> Aug, 2025; Revised: 28<sup>th</sup> Oct 2025; Accepted: 16<sup>th</sup> Nov, 2025; Available Online: 1<sup>st</sup> December, 2025

## ABSTRACT

Novel gastroretentive drug delivery systems in the form of superporous hydrogels were developed to achieve prolonged epigallocatechin gallate (EGCG) delivery. The optimized formulation was composed of 2% w/w chitosan, 2% w/w poly(vinyl alcohol), and 0.3% w/w glyoxal. It displayed rapid swelling within 5 minutes of immersion in 0.1 N hydrochloric acid (pH 1.2) and exhibited a gradual release of more than 80% of EGCG over 8 hours. The superporous hydrogels exhibited high compressive strength, suggesting resistance to the contractile pressure in the stomach. The degradation kinetics of the systems depended on the contents of chitosan and PVA. The optimized formulation significantly reduced nitric oxide (NO) production in LPS-stimulated RAW 264.7 macrophage cells and exhibited moderate anti-inflammatory activity. These results suggest that the superporous hydrogel could serve as an effective alternative delivery system for herbal anti-inflammatory agents.

**Keywords:** Epigallocatechin Gallate, Gastroretentive Drug Delivery System, Superporous Hydrogel

**How to cite this article:** Lakhiew A, Preparatana R, Issarachot O, Wiwattanapatapee R, Development of Biodegradable Superporous Hydrogels for Gastroretentive Delivery of Epigallocatechin Gallate. *Int J Drug Deliv Technol.* 2026;16(1): 388-402. DOI: 10.25258/ijddt.16.1.42

**Source of support:** Financial support from the Project of Strengthening Excellence in Pharmacy, Faculty of Pharmaceutical Sciences, Prince of Songkla University.

**Conflict of interest:** None

## INTRODUCTION

Gastroretentive drug delivery systems (GRDDS) have been developed to overcome the drawbacks of conventional oral dosage forms, whose retention time in the stomach depends on the stages of gastric motility [1]. The efficiency of drugs and active substances administered via the oral route is often reduced by several gastrointestinal factors, such as metabolism by gastrointestinal enzymes, unfavorable environments, or instability in the alkaline conditions of the gastrointestinal tract (GIT), which together lead to decreased drug absorption [2]. Furthermore, certain physicochemical properties of drugs such as a short half-life, poor absorption, and low solubility at the higher pH of the intestine—can further limit their therapeutic efficacy [3]. To overcome these limitations, GRDDS have been invented to prolong the gastric residence time of drugs. These systems employ several strategies, including low-density systems [4], high-density systems [5], expandable systems [6], raft-forming systems [7], and superporous hydrogels [8].

Superporous hydrogels (SPHs) have been developed based on the concept of forming a three-dimensional polymer network. The rapid swelling occurs in short time of contact to aqueous solution by the interconnected pores surrounding the systems [9]. The floating ability allows the

system to be retained longer in the stomach, combined with its larger dimensions that prevent pyloric passage. The drug-carrying ability of these systems is of interest for targeted drug delivery, particularly in the stomach, to prolong drug release and increase bioavailability [10]. To optimize the SPHs, the type and content of polymers and excipients can be selected to achieve suitable SPHs capable of carrying the drug and prolonging its release over time. Chitosan, a natural linear polysaccharide derived from the deacetylation of crustacean chitin [11], is a polymer that can be utilized in superporous hydrogels due to its hydrophilic nature and high swelling ability in acidic environments [12]. Because of the fragile mechanical strength of first-generation SPHs produced from acrylic-type monomers, the addition of chitosan as a hybrid agent can improve the mechanical strength owing to the cross-linking reaction that occurs after the system is formed [13]. Furthermore, the SPH hybrid systems possess a unique property in that the gels are highly elastic in the swollen state, making them hardly breakable in aqueous solution when stretched [14]. Consequently, the incorporated drug can be released in a controlled manner, which is beneficial for sustained drug release.

Epigallocatechin gallate (EGCG) is the predominant polyphenolic compound found in *Camellia sinensis* (green

\*Author for Correspondence: ruedeekorn.w@psu.ac.th.

tea). Its therapeutic activities have attracted interest for both treatment and prophylaxis. These include antioxidant, anti-inflammatory, and anti-tumor properties [15]. Moreover, EGCG has the ability to modulate cell signaling pathways related with apoptosis, immune regulation, and oxidative stress that are beneficial for health [16]. However, the oral bioavailability of EGCG is relatively low due to extensive metabolism by gut microbiota and its instability in the intestinal environment [2]. Therefore, prolonging the gastric retention time of EGCG in the stomach may enhance its absorption and overall bioavailability.

To deliver EGCG to the stomach, chitosan-based superporous hydrogels were prepared using the gas-blowing technique. Poly(vinyl alcohol) (PVA), a synthetic polymer, was incorporated as a monomer due to its hydrophilicity and biocompatibility, and its potential biodegradability under specific conditions. Moreover, PVA enhances the mechanical strength of the SPHs owing to its ability to form stable networks through various cross-linking mechanisms [17]. Although numerous studies have employed synthetic polymers, such as polyacrylamide or poly(AA-co-AM), for the preparation of SPHs, there is limited research on the combined use of PVA and chitosan as a drug carrier in SPH systems. Investigating the effects of polymer composition and formulation excipients is therefore essential to develop an optimized system capable of achieving sustained gastric release of EGCG [18].

This study presents the preparation of chitosan- and PVA-based SPHs using glyoxal as a cross-linking agent and sodium bicarbonate as a poring agent. The gas-blowing technique was employed to form the SPHs, and lyophilization was used for drying. The samples were characterized for their physicochemical properties, including porosity, density, mechanical strength, water absorption capacity, and stability in gastric conditions. The drug release profiles were evaluated to investigate the sustained release of EGCG in gastric fluid and to elucidate the underlying release mechanism. Additionally, the bioactivities of EGCG, including its antioxidant and anti-inflammatory effects, were assessed.

## 2. MATERIALS AND METHODS

### 2.1 Material

EGCG powder (98%) was purchased from Xi'an Nate Biological Technology (China). White chitosan (Molecular weight 500,000, degree of deacetylation 85%) was acquired from BIO21 (Samutsakhon, Thailand) Polyvinyl alcohol (PVA, Molecular weight 30,000 – 70,000), and glyoxal solution (40 %) was obtained from Sigma (St. Louise, MO, USA). Konjac glucomannan (KGM) Extract Powder was sourced from Asia Bioplex (Chonburi, Thailand). Fibroblast (3T3-L1), and murine macrophage cell line (RAW264.7) were acquired from the American Type Culture Collection, ATCC (VA, USA). Fetal calf serum (FCS) was purchased from Gibco (Invitrogen, California, USA). Penicillin-streptomycin obtained from Invitrogen (Invitrogen, California, USA). Lipopolysaccharide (LPS, from *Escherichia coli*), 3-(4,5-

dimethyl-2-thiazolyl)-2,5-diphenyl-2H-tetrazolium bromide (MTT), Roswell Park Memorial Institute 1640 (RPMI-1640) medium, Dulbecco's modified Eagle's medium (DMEM), indomethacin and phosphate buffer saline (PBS) were obtained from Sigma Aldrich (Sigma Aldrich, Missouri, USA). All other chemical were analytical grades.

### 2.2 Preparation of superporous hydrogel

The components of the SPHs formulation are shown in Table 1. SPHs were prepared by the gas-foaming method with some modifications, as previously described [19,20]. In brief, chitosan was dissolved in 1 M acetic acid, while PVA and KGM were separately dissolved in deionized water at varying concentrations. The chitosan solution was then added to the PVA solution, and the mixture was stirred until completely dissolved. For formulations A14–A16, the PVA solution was first mixed with the KGM solution, followed by the addition of the chitosan solution. EGCG was then incorporated into the mixture, which was homogenized at 1000 rpm for 5 min to obtain a smooth solution. Next, glyoxal solution (40%) was added as a cross-linking agent. Sodium bicarbonate was subsequently added as a poring agent to create the porous structure within the hydrogel, and the mixture was stirred until uniform. The final solution was poured into 24-well plates and frozen at  $-20^{\circ}\text{C}$  overnight. Superporous hydrogels were obtained by lyophilization using a freeze dryer (Lyovapor L-300, Buchi, Flawil, Switzerland). The resulting samples were stored in a desiccator until further physicochemical characterization.

**Table 1. Composition of superporous hydrogel formulations**

Formulation	% w/w				Sodium bicarbonate (mg)	EGCG (mg)
	Chitosan	PVA	KGM	Glyoxal		
A1	2	2	-	0.1	100	50
A2	2	2	-	0.3	100	50
A3	2	2	-	0.5	100	50
A4	2	3	-	0.3	100	50
A5	2	4	-	0.3	100	50
A6	2	5	-	0.3	100	50
A7	2	2	-	0.3	50	50
A8	2	2	-	0.3	200	50
A9	2	2	-	0.3	100	75
A10	2	2	-	0.3	100	100
A11	1	1	-	0.3	100	50
A12	2	1	-	0.3	100	50
A13	3	1	-	0.3	100	50
A14	2	1	1	0.3	100	50
A15	2	1	2	0.3	100	50
A16	2	1	3	0.3	100	50

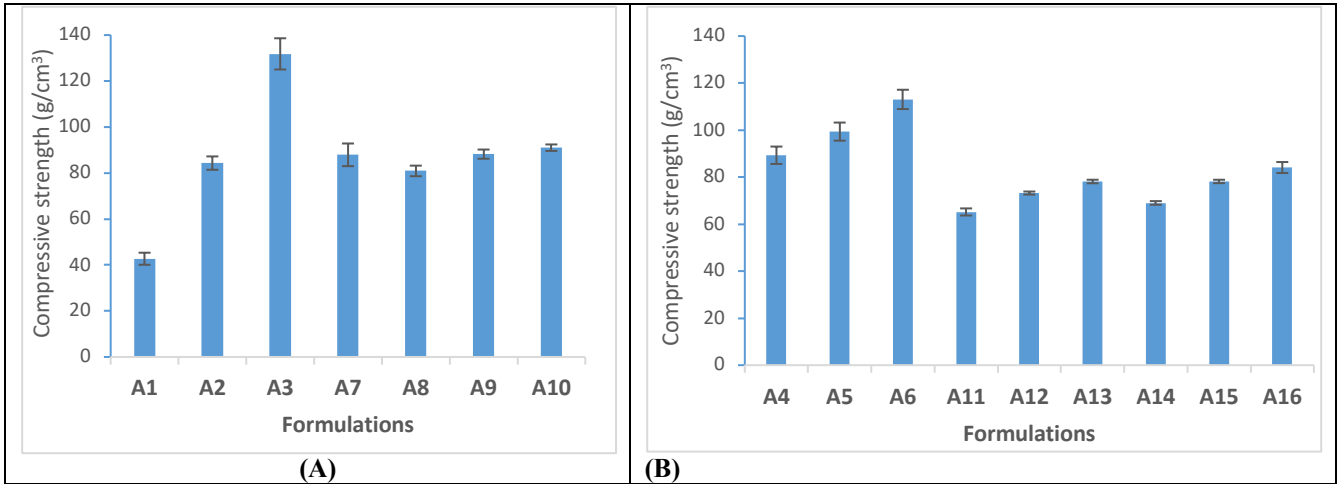


Figure 1. Compressive strength of superporous hydrogel formulations.

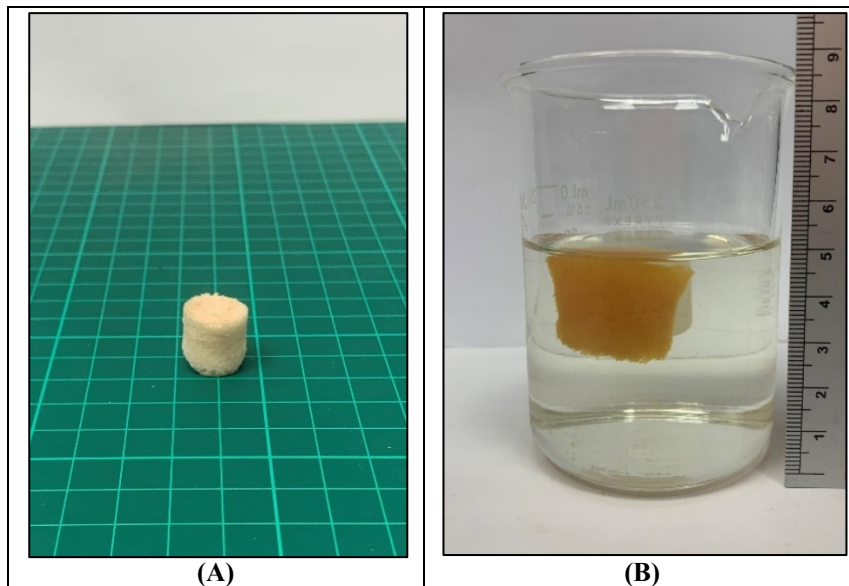


Figure 2. Characteristics of (A) dried stage, and (B) swollen stage of superporous hydrogel (formulation A12)

**2.3 Physicochemical characterization of EGCG-loaded superporous hydrogel**

**2.3.1 Average weight**

Each EGCG-loaded superporous hydrogel sample was retrieved from 48-well plates. Ten samples were weighed using an analytical balance (XB 220 A, Precisa, Dietikon, Switzerland). The average weight, thickness, and standard deviation (SD) were calculated and reported ( $n = 5$ ).

**2.3.2 Density measurement**

The density of dried EGCG-loaded superporous hydrogels was determined using the solvent displacement method. Each sample, in triplicate, was weighed and placed in a graduated cylinder containing hexane. The density of the EGCG SPHs was calculated using the following equation:

$$\text{Density} = m/v \tag{1}$$

Where  $m$  is mass of dried EGCG SPHs, and  $v$  is the volume increase of hexane ( $n = 3$ )

**2.3.3 Porosity measurement**

The percentage porosity of the superporous hydrogels was determined using the solvent replacement method. Dried samples were immersed in absolute ethanol overnight, after which excess ethanol on the surface was gently blotted. The samples were then weighed, and porosity was calculated using the following equation:

$$\text{Porosity} = (M2 - M1/\rho V) \tag{2}$$

Where  $M1$  and  $M2$  are the weight of hydrogel before and after immersion in absolute ethanol, respectively;  $\rho$  is the density of absolute ethanol, and  $V$  is the volume of the hydrogel ( $n = 3$ ).

**2.3.4 Strength measurement**

The compressive strength of the samples was determined using a texture analyzer (Stable Micro Systems, Scardale, NY, USA). Cylindrical superporous hydrogels in the dried state were first swollen in 0.1 N HCl solution and measured at equilibrium. The samples were compressed using a

\*Author for Correspondence: ruedeekorn.w@psu.ac.th.

cylindrical probe with the pre-test condition of speed 2.0 mm/sec, test speed of 1.0 mm/sec, and post-test speed of 2.0 mm/sec. the maximum force was recorded and average values of triplicate tests of each sample were reported ( $n = 5$ ).

### 2.3.5 Water absorption capacity

The water absorption capacity of the superporous hydrogels was evaluated through a swelling study in simulated gastric fluid (pH 1.2). Cylindrical hydrogel samples were initially weighed ( $W_1$ ) and then immersed in the fluid at room temperature. At predetermined time intervals (2.5, 5, 10, 15, 30, 60, 120, 240, and 480 min), the samples were removed and their increased weight ( $W_2$ ) was measured using an analytical balance. The percentage of weight increase was calculated using the following equation ( $n = 3$ ).

$$\text{Water absorption (\%)} = [(W_2 - W_1) / W_1] \times 100 \quad (3)$$

### 2.3.6 In vitro release of EGCG from superporous hydrogel

The release behavior of EGCG was examined using a USP dissolution apparatus II (paddle) at 100 rpm. The samples were placed in the 900 mL of simulated gastric fluid 0.1 N HCl, pH 1.2 as a dissolution medium,  $37^\circ\text{C} \pm 0.5^\circ\text{C}$ . at the determined time intervals of 5, 10, 15, 30 min, and 1, 2, 4, and 8 h, Samples were collected for 5 mL to analyze followed by replacing the same volume of fresh dissolution medium. The amount of EGCG were quantitatively analyzed by UV-vis spectroscopy at 274 nm. Each formulation was examined in triplicate.

### 2.3.7 Release kinetics of EGCG

The EGCG release profile from the superporous hydrogels was analyzed by plotting the cumulative release data obtained in pH 1.2 medium and fitting it to various mathematical models of drug release, including zero-order [19], first-order [20], Hixson-Crowell [21], Higuchi [22], and Korsmeyer-Peppas models [23].

### 2.3.8 Determination of drug content

The EGCG-loaded superporous hydrogel formulations were analyzed for drug content by extracting EGCG into 100 mL of deionized water in a volumetric flask. Samples were sonicated for 6 h and then shaken at  $40^\circ\text{C}$  for 24 h to ensure complete dissolution of EGCG from the hydrogel. The solution was filtered through a  $0.45 \mu\text{m}$  nylon filter, and the drug concentration was determined using UV-Vis spectrophotometry at a wavelength of 274 nm. Entrapment efficiency was calculated ( $n = 5$ ).

### 2.3.9 Erosion determination

The erosion of superporous hydrogels over time was investigated following the procedure described by Avachat and Kotwal (2007) [24]. In brief, cylindrical hydrogel samples of uniform shape were selected and placed in a USP dissolution vessel containing 1000 mL of 0.1 N HCl solution (pH 1.2). The vessel was stirred using a USP apparatus II paddle at 100 rpm and maintained at  $37 \pm 0.5^\circ\text{C}$ . Samples were withdrawn at predetermined time intervals (0.5, 1, 2, 3, 4, 6, 8, 12, 24, and 48 h) and dried in an oven at  $40^\circ\text{C}$  until constant weight was achieved. The percentage of erosion was calculated using the following equation:

$$E = (W_i - W_f) / W_i \times 100 \quad (4)$$

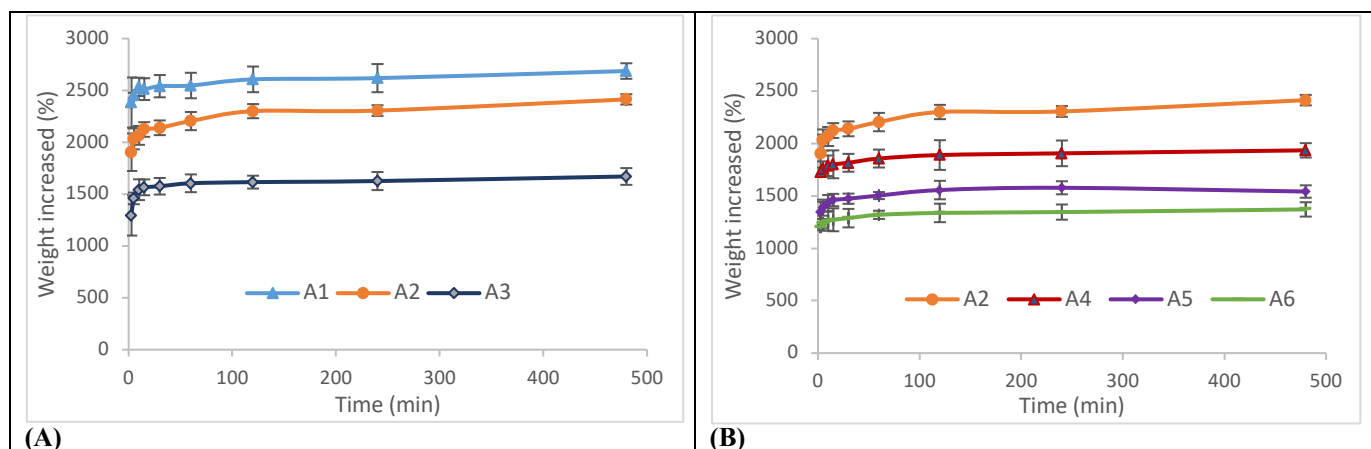
$W_i$  and  $W_f$  are the dried weights of the initial and the intervals time point collected, respectively ( $n = 5$ ).

### Fourier transform infrared (FT-IR) studies

FTIR spectroscopy was performed by collecting the FTIR spectra between the wavenumber range of  $450\text{--}4000 \text{ cm}^{-1}$  using a PerkinElmer 400 instrument. KBr and the samples were compressed for scanning to categorize the functional groups present in excipients of the superporous hydrogel.

### Morphology

Superporous hydrogel was examined for the morphology by scanning electron microscopy technique (SEM, Quanta 400, FEI, USA). The formulation was coated and analyzed at an accelerating voltage of 20 keV.



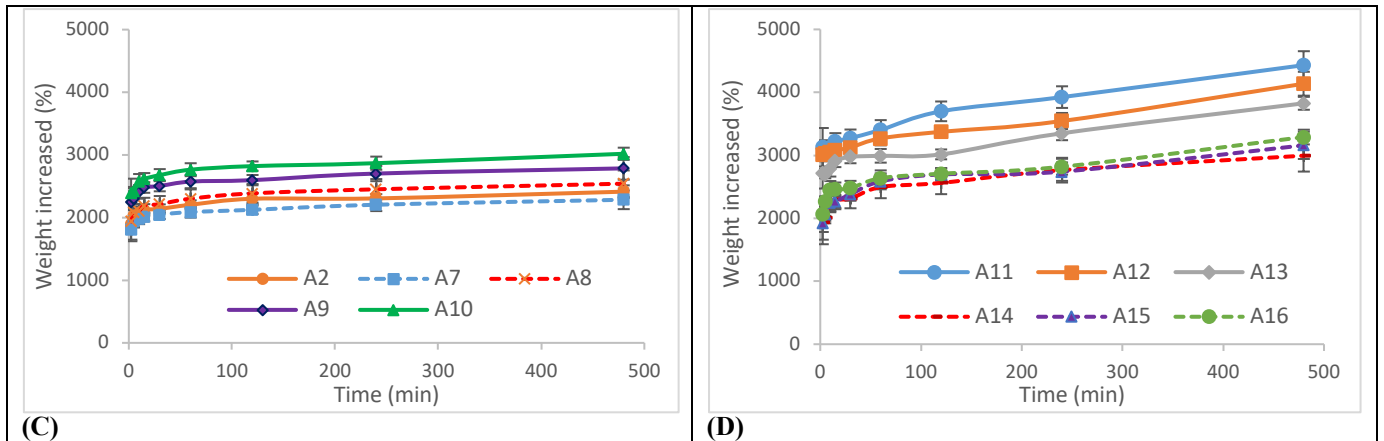


**Figure 3. Water absorption capacity of superporous hydrogels: (A) Difference in crosslinking agent content (A1-A3); (B) difference in PVA content (A4-A6, compared to A2); (C) Difference in poring agent content and drug loading (A7-A10); (D) Difference in chitosan and KGM content (A11-A16) (n = 3, mean ± SD).**

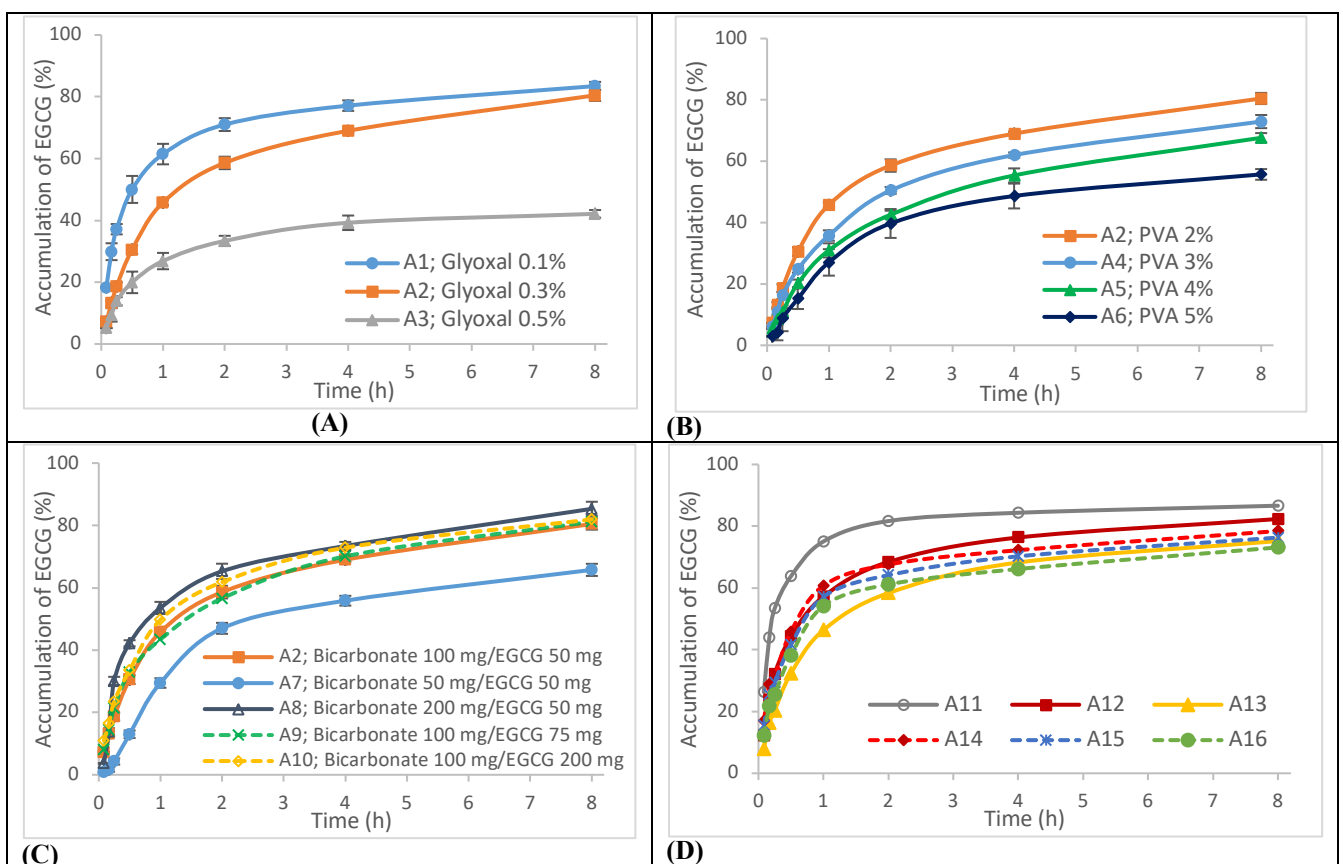


**Figure 4. Drug release profile in SGF pH 1.2 of superporous hydrogels: (A) Difference in crosslinking agent content (A1-A3); (B) difference in PVA content (A4-A6, compared to A2); (C) Difference in poring agent content and drug loading (A7-A10); (D) Difference in chitosan and KGM content (A11-A16) (n = 3, mean ± SD).**

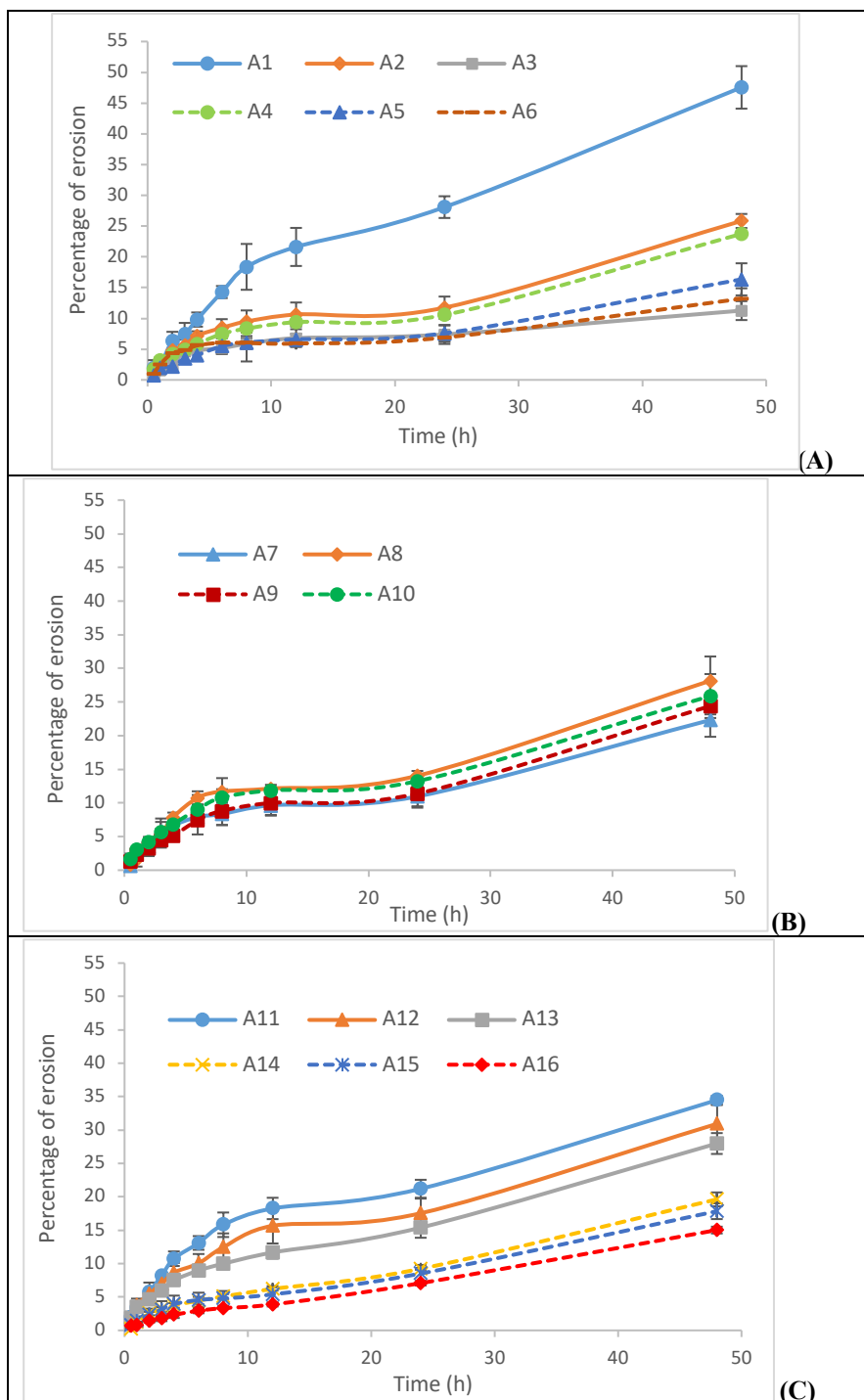


Figure 5. Percentage erosion of superporous hydrogel formulations after 48 h: (A) formulation A1–A6; (B) formulation A7–A10; (C) formulation A11–A16

## 2.4 Evaluation of biological activities

### 2.4.1 Determination of antioxidant activity

A 0.1 mM 2,2-diphenyl-1-picrylhydrazyl (DPPH) solution was arranged by dissolving DPPH powder in 99% methanol and incubating in the dark. The 96-well plates were added by a 100  $\mu$ L aliquot of this solution and mixed with 300  $\mu$ L of EGCG formulations at six concentrations of 3.13, 6.25, 12.5, 25, 50, and 100  $\mu$ g/mL. Ascorbic acid, and

blank samples were prepared at the same concentrations to compare the activities as a reference compound. Prior to the measurement, the mixtures were incubated in the dark for 30 min. The UV absorbance was determined at 517 nm using a microplate reader, and the free radical scavenging activity was calculated using the following equation. All experiments were performed in triplicate ( $n = 3$ ).

$$\text{Radical scavenging activity (\%)} = \left[ 1 - \left( \frac{B}{A} \right) \right] \times 100 \quad (5)$$

Where A represents the absorbance of methanol without sample (control), and B represents the absorbance of the sample.

#### 2.4.2 *In vitro* cytotoxic and anti-inflammatory activity

##### 2.4.2.1 *In vitro* cytotoxicity test on macrophage cells

Cytotoxicity on RAW264.7 macrophage cell line was evaluated by MTT-assay technique. The cells were seeded in a 96-well plate and cultured for 12-16 h to obtain a density of 80,000 cells/well. Five concentrations (100, 50, 25, 12.5, and 6.25  $\mu\text{g/mL}$ ) of EGCG formulations, EGCG standard, blank, and indomethacin (positive control) were then treated to the cultured cells, followed by a 24 h incubation. Subsequently, MTT solution (concentration 5 mg/mL) was diluted (1:20) in medium. Obtained MTT solution of 100  $\mu\text{L}$  was added to each well containing the macrophage cells. The cells were further incubated for 2 h after which the supernatant was removed, formazan crystals were dissolved by adding 200  $\mu\text{L}$  of dimethyl sulfoxide (DMSO) to each well. The absorbance at 570 nm was examined using a microplate reader (Biotek model PowerWave X, Santa Clara, CA, USA). The percentage of cell viability was calculated according to the equation (6). Additionally,  $\text{IC}_{50}$  values were denoted as the concentration of the sample at which 50% of cell viability is inhibited.

$$\text{Cell viability (\%)} = \left[ \frac{A_{\text{sample}}}{A_{\text{control}}} \right] \times 100 \quad (6)$$

Where  $A_{\text{control}}$  and  $A_{\text{sample}}$  signify the absorbance of control and the test sample, respectively ( $n = 3$ ).

##### 2.4.2.2 *Anti-inflammatory activity assay*

Inhibition of nitric oxide (NO) production in RAW264.7 macrophage cell line was assessed for anti-inflammatory

activity. Cells were grown in RPMI 1640 medium supplemented 10% fetal bovine serum (FBS), 2 mM L-glutamine, 100 units/mL penicillin G, 100  $\mu\text{g/mL}$  streptomycin, and 0.1% sodium bicarbonate. The cells were seeded in a 96-well plate and further incubated at 37  $^{\circ}\text{C}$  under a 5%  $\text{CO}_2$  atmosphere for 12 h to obtain a density of 80,000 cells/well. Five concentrations of the samples (100, 50, 25, 12.5, and 6.25  $\mu\text{g/mL}$ ) were then treated to cells exposed to lipopolysaccharide (LPS) to induce inflammation activities compared to the RAW 264.7 cells without being induced by LPS as the negative control, followed by a 24-hour incubation. Griess reagent was utilized to quantify NO production represented by nitrite levels in the culture medium. The absorbance was measured at 570 nm using a microplate reader (Biotek model PowerWave X, Santa Clara, CA, USA), with indomethacin as the positive control ( $n = 3$ ).

#### 2.5 Statistical analysis

The data are represented as the mean  $\pm$  SD of triplicate or independent experiments. Data analysis was executed by Student's t-test and one-way ANOVA. Statistical probability ( $p$  values) of  $< 0.05$  or  $< 0.01$  were considered statistically significant.

### 3. RESULTS AND DISCUSSION

#### 3.1 Characterization of EGCG-loaded superporous hydrogel

##### 3.1.1 Average weight of SPHs

As represent in Table 2, the weight of the EGCG SPHs was between  $0.103 \pm 0.013$  and  $0.195 \pm 0.012$  g, depending on the content of polymers and drug loading. The standard deviation of all formulations was lower than 5.0%, indicating the reproducibility and acceptability of the preparation method. All data were obtained from 5 repeated samples.

**Table 2 Characterization of EGCG-loaded superporous hydrogels in terms of weight, density, porosity, and drug content**

Formulations	Weight (g)	Density (g/ml)	Porosity (%)	drug content (%)
A1	$0.127 \pm 0.011$	$0.654 \pm 0.031$	$75.51 \pm 1.52$	$100.86 \pm 4.58$
A2	$0.168 \pm 0.009$	$0.718 \pm 0.013$	$68.66 \pm 0.95$	$96.05 \pm 2.03$
A3	$0.179 \pm 0.008$	$0.783 \pm 0.018$	$62.19 \pm 1.24$	$87.21 \pm 3.29$
A4	$0.179 \pm 0.006$	$0.728 \pm 0.014$	$69.00 \pm 0.23$	$96.15 \pm 1.30$
A5	$0.183 \pm 0.006$	$0.758 \pm 0.019$	$69.34 \pm 0.29$	$94.80 \pm 2.06$
A6	$0.195 \pm 0.012$	$0.795 \pm 0.017$	$69.90 \pm 0.42$	$94.70 \pm 1.35$
A7	$0.170 \pm 0.006$	$0.734 \pm 0.036$	$67.11 \pm 0.42$	$93.01 \pm 1.77$
A8	$0.166 \pm 0.007$	$0.720 \pm 0.012$	$69.60 \pm 1.36$	$97.96 \pm 3.94$
A9	$0.172 \pm 0.009$	$0.735 \pm 0.015$	$65.68 \pm 0.30$	$95.81 \pm 3.32$
A10	$0.177 \pm 0.012$	$0.768 \pm 0.012$	$64.38 \pm 0.16$	$94.29 \pm 2.48$
A11	$0.103 \pm 0.013$	$0.613 \pm 0.021$	$73.99 \pm 0.12$	$99.67 \pm 1.89$
A12	$0.143 \pm 0.009$	$0.661 \pm 0.015$	$71.29 \pm 0.18$	$98.64 \pm 3.54$
A13	$0.155 \pm 0.012$	$0.722 \pm 0.037$	$68.40 \pm 0.12$	$95.90 \pm 3.41$
A14	$0.129 \pm 0.012$	$0.695 \pm 0.029$	$70.75 \pm 0.22$	$97.68 \pm 1.27$
A15	$0.149 \pm 0.008$	$0.724 \pm 0.021$	$70.34 \pm 0.26$	$95.06 \pm 3.47$
A16	$0.162 \pm 0.015$	$0.761 \pm 0.021$	$67.74 \pm 0.16$	$94.00 \pm 2.33$

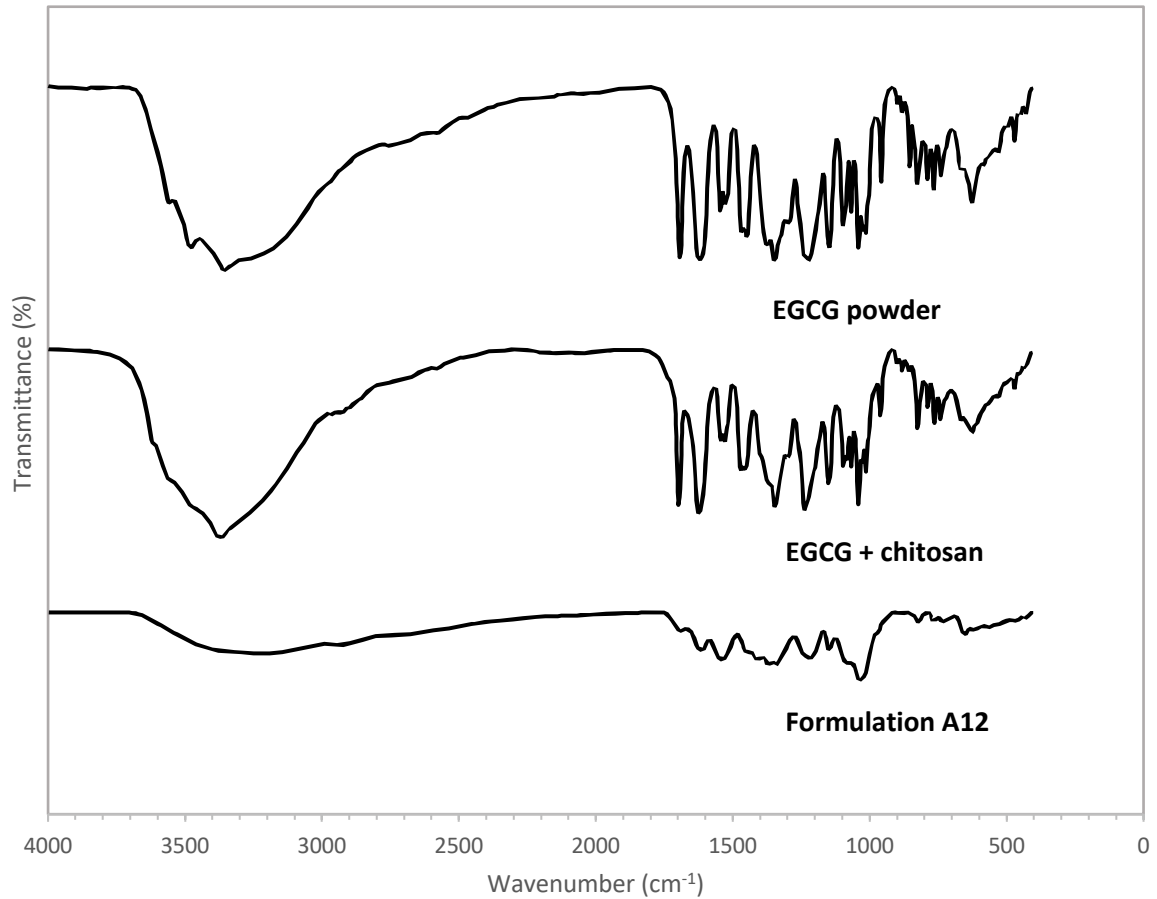


Figure 6. FTIR analysis of EGCG powder, Mixture (EGCG and chitosan), and superporous hydrogel (Formulation A12)

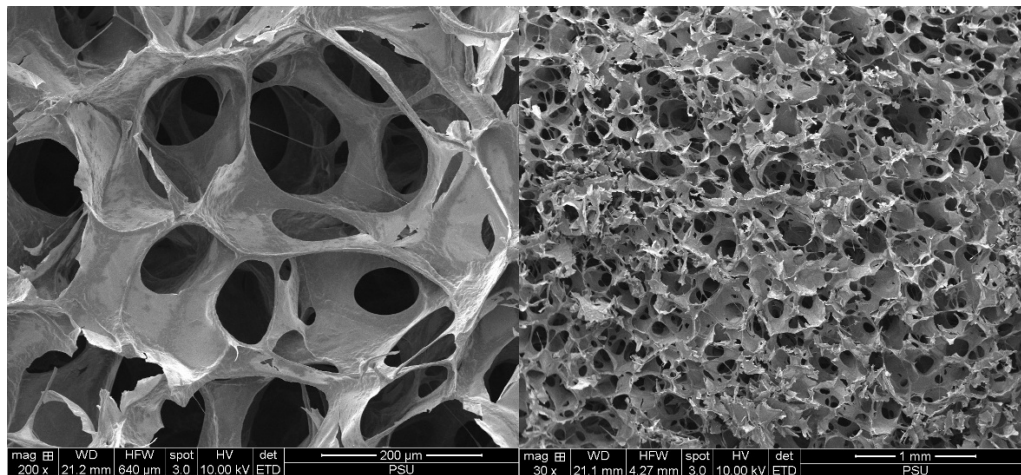
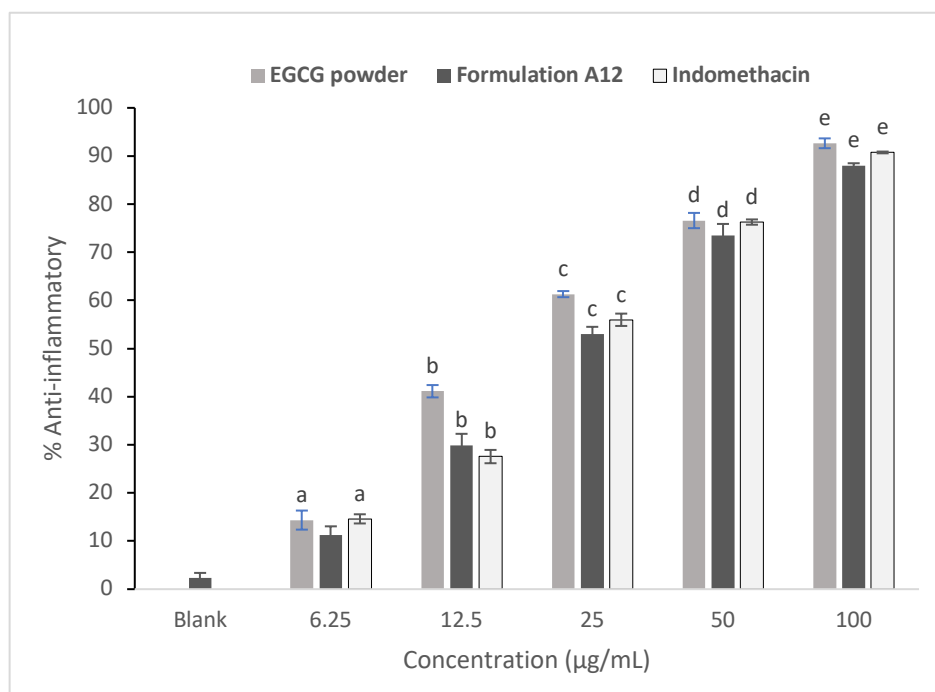


Figure 7. SEM photograph of dried superporous hydrogels (formulation A12) at different views and magnifications showing interconnected pores. (left) cross-section (x200), (right) surface (x30)



**Figure 8.** Anti-inflammatory effect, measured by NO reduction in LPS-induced RAW 264.7 cells of varying concentrations of EGCG standard powder and Formulation A12, compared with indomethacin ( $n = 3$ , mean  $\pm$  standard deviation). <sup>a</sup>statistically significant differences compared to blank formulation ( $p < 0.05$ ); <sup>b</sup>compared to EGCG power concentration of 6.25  $\mu\text{g/mL}$  ( $p < 0.05$ ); <sup>c</sup>compared to A12 formulation with EGCG concentration of 12.5  $\mu\text{g/mL}$  ( $p < 0.05$ ); <sup>d</sup>compared to A12 formulation with EGCG concentration of 25  $\mu\text{g/mL}$  ( $p < 0.05$ ); <sup>e</sup>compared to A12 formulation with EGCG concentration of 50  $\mu\text{g/mL}$  ( $p < 0.05$ ).

### 3.1.2 Density measurement

The apparent density of EGCG SPHs ranged from  $0.613 \pm 0.021$  to  $0.795 \pm 0.017$  g/mL, which was lower than that of gastric fluid (1.004 g/mL), suggesting that they might possess buoyant properties that could prolong their gastric retention time in the stomach. The lowest apparent density of formulation A11 was attributed to its low polymer content, as increasing the polymer concentration resulted in a higher apparent density. This could be explained by the enhanced strength of the polymeric network at higher polymer levels, which reduced gas expansion due to the increased resistance force [9]. The increase in density was not only dependent on the contents of chitosan and PVA, but also on the higher KGM content. The increase in density from  $0.654 \pm 0.031$  to  $0.783 \pm 0.018$  g/mL as the crosslinking agent concentration increased from 0.1% to 0.5% could be attributed to the formation of chitosan–PVA conjugates after polymer crosslinking, which increased the weight per unit volume of the system, resulting in higher density. Moreover, the greater mechanical strength of the crosslinked SPHs may have restricted gas expansion and limited dimensional changes in the hydrogels [8]. In contrast, EGCG loading caused only a slight change in the apparent density.

### 3.1.3 Porosity measurement

The porosity of the formulations, determined by the solvent displacement method, ranged from  $62.19 \pm 1.24\%$  to  $75.51 \pm 1.52\%$ . These two extreme values corresponded to the reduction of glyoxal content from 0.5% to 0.1%, indicating that porosity increased as the concentration of the

crosslinking agent decreased. Gupta *et al.* (2010) reported that the conjugation between chitosan and the crosslinking agent decreased the occupied volume of the hydrogels, as the crosslinking agent promoted stronger interactions or attachments between polymer chains. Furthermore, the reduction in occupied volume can influence the swelling ability of the hydrogels to absorb aqueous solutions [25]. In addition, increasing the polymer content was associated with a decrease in porosity. As the chitosan content increased from 1%, 2%, to 3% in formulations A11, A12, and A13, the porosity decreased from  $73.99 \pm 0.12\%$  to  $71.29 \pm 0.18\%$  and  $68.40 \pm 0.12\%$ , respectively. Chevda *et al.* (2009) explained that a lower chitosan content facilitates the formation of larger gas bubbles within the mixture, resulting in larger pore sizes in the hydrogel due to reduced chitosan accumulation at the pore periphery. Conversely, higher chitosan concentrations introduce excessive water into the system, leading to the collapse of some bubbles and, consequently, a reduction in hydrogel porosity [26]. Similar to the effect of chitosan content, the combined increase of KGM and PVA also exhibited a decreasing trend in porosity.

### Strength measurement

A gastroretentive drug delivery system must be capable of withstanding gastric contraction pressure. SPHs containing 2% PVA and 2% chitosan were prepared with varying glyoxal concentrations (0.1%, 0.3%, and 0.5%) to examine the effect of crosslinking density. As shown in Fig. 1A, formulation A3 (0.5% glyoxal) exhibited the highest compressive strength ( $131.82 \pm 6.79$  g/cm<sup>3</sup>), followed by A2 ( $84.32 \pm 2.91$  g/cm<sup>3</sup>), indicating that increased

crosslinking enhanced mechanical strength. In contrast, formulation A1 (0.1% glyoxal) showed the lowest strength ( $42.72 \pm 2.63 \text{ g/cm}^3$ ) due to insufficient crosslink formation within the hydrogel network. The addition of sodium bicarbonate (A7, A8) and EGCG loading (A9, A10) produced only minor variations in compressive strength. The compressive strength was also influenced by the polymeric network composition, particularly the concentrations of chitosan, PVA, and the crosslinking agent. Increasing the PVA content (formulations A4, A5, and A6 containing 3%, 4%, and 5% PVA with 2% chitosan, respectively; Fig. 1B) enhanced the mechanical strength of the hydrogels from  $89.30 \pm 6.79$  to  $99.36 \pm 3.85$  and  $113.06 \pm 4.11 \text{ g/cm}^3$ , demonstrating the effect of polymer concentration on mechanical properties. Similarly, increasing chitosan content from 1% to 3% (formulations A11–A13, each containing 1% PVA) raised the compressive strength from  $65.18 \pm 1.51$  to  $73.22 \pm 0.65$  and  $78.14 \pm 0.75 \text{ g/cm}^3$ , respectively. A comparable trend was observed with increasing KGM content (formulations A14–A16), where compressive strength values increased from  $69.02 \pm 0.77$  to  $78.16 \pm 0.72$  and  $84.08 \pm 2.34 \text{ g/cm}^3$ , respectively. Overall, the results indicate that the compressive strength of SPHs was primarily governed by the crosslinking agent content, followed by the polymer type and concentration.

### 3.1.5 Water absorption capacity

The hydrogels rapidly absorbed the swelling medium under acidic conditions. The superporous hydrogel structure, containing numerous pores that form capillary channels, facilitated the diffusion of the medium into the polymeric matrix. The characteristics of the hydrogels in the dried and swollen states are shown in Fig. 2. As illustrated in Fig. 3, all SPH formulations exhibited rapid swelling upon contact with simulated gastric fluid, with a weight gain of approximately 1500% of the initial weight. Subsequently, the hydrogels reached an equilibrium state, which was maintained for up to 4 hours.

#### Effect of crosslinking-agent concentration

The effect of glyoxal content on formulations A1, A2, and A3 was evaluated. A low glyoxal concentration in formulation A1 (0.1%) resulted in a higher percent weight increase, whereas higher glyoxal concentrations in formulations A2 (0.3%) and A3 (0.5%) reduced the water absorption capacity of the hydrogels. This phenomenon can be attributed to the increased strength of the hydrogel network, which limits its swelling ability [27]. As shown in Fig. 3A, the percent weight increase of A3 was 1,670.2%, compared with 2,686.9% for A1 and 2,413.4% for A2. Thus, higher glyoxal content enhanced hydrogel rigidity through greater crosslinking, leading to reduced swelling capacity.

#### Effect of PVA concentration

To evaluate the effect of PVA, chitosan and crosslinker contents were kept constant while PVA was varied from 2% to 5% in formulations A2, A4, A5, and A6. Increasing PVA content reduced hydrogel swelling and weight gain, as higher PVA levels enhanced gel strength but limited water absorption. This effect can be attributed to the resistance to

expansion caused by the stronger polymeric network [28]. Swelling is facilitated by hydrogen bonding between water molecules and hydrophilic functional groups, such as amino and hydroxyl groups on chitosan chains, which promote fluid penetration into the network. In formulations A11–A13, reducing PVA to 1% (A7) markedly increased hydrogel swelling (~2,000%), indicating that 1% PVA is sufficient to maintain structural integrity while sustaining EGCG release for up to 8 hours.

#### Effect of chitosan concentration

Chitosan content was increased from 1% to 3% in formulations A11, A12, and A13, respectively. Higher chitosan levels resulted in reduced hydrogel swelling, as indicated by the decreasing swelling percentages from A11 to A13. This behavior can be explained by polymer–water interactions: hydrophilic groups, such as amides, initially bind water molecules through hydrogen bonding until equilibrium swelling is reached, after which free water fills the voids and pores within the network [29]. Similarly, Cen *et al.* (2023) reported that small amounts of chitosan incorporated into cellulose-based copolymer films enhanced both tensile strength and plasticity. In addition, capillary action contributes to rapid fluid uptake beyond simple absorption. The increase in void space is also linked to the ionization of amine groups in chitosan, which convert to ammonium ions under acidic conditions [30]. This ionization generates electrostatic repulsion within the polymer network, expanding the structure and further enhancing fluid uptake.

#### Effect of Konjac glucomannan concentration

Formulations A14–A16 were SPHs prepared with 1–3% KGM in combination with 2% chitosan and 1% PVA. The swelling behavior increased with higher KGM content, as indicated by weight gain percentages of 3158.62% (A14), 3324.40% (A15), and 3490.16% (A16). These results suggest that KGM has a weaker influence on SPH swelling compared to chitosan (A11–A13). The enhanced water absorption with increasing KGM content is attributed to the acetyl groups in its structure, which play a key role in its hydrophilicity and gelation properties [31]. Yui *et al.* (1992) reported that KGM chains adopt an extended two-fold helical conformation, stabilized primarily by intermolecular O–3–O–5 hydrogen bonding and rotational interactions around C–6. X-ray diffraction analysis further demonstrated that variations in acetyl substitution influence KGM's structural organization. According to the theory of network integration, KGM can form left- and right-handed single-helical three-stage structures in aqueous solution, with hydrogen bonding serving as the dominant stabilizing force [32].

#### Effect of poring agent

Sodium bicarbonate was incorporated into the SPHs as a poring agent. Formulations A7 and A8 contained 50 mg and 200 mg, respectively, resulting in fluid uptake of 2284.4% and 2541.2%. The increased fluid uptake can be explained by Ghazali *et al.* (2017), who reported that the swelling ratio of SPHs increases with the concentration of foaming or poring agents up to an optimum level. Sodium bicarbonate

promotes pore formation within the hydrogel structure, thereby enhancing water absorption [33].

#### Effect of drug loading

Increasing the EGCG loading in SPHs from 50 mg to 75 mg (A9) and 100 mg (A10) resulted in higher fluid uptake, reaching 2785.2% and 3018.2%, respectively, compared to formulation A2 (50 mg). This behavior can be explained by Ding *et al.* (2025), who reported that higher EGCG content in hydrogel-based wound dressings decreased the storage modulus ( $G'$ ) of the gels. This suggests that increased EGCG weakens the hydrogel network, enhancing water absorption due to its hindering effect on crosslinking within the hydrogel matrix [34].

#### 3.1.6 *In vitro* release of EGCG from superporous hydrogel

The *in vitro* release profiles of EGCG-loaded SPHs in pH 1.2 HCl solution over 8 hours are shown in Fig. 4. As illustrated in Fig. 4A, the glyoxal content significantly influenced drug release. Formulation A1, containing 0.1% glyoxal, exhibited the highest release, reaching 80% over 8 hours. In contrast, increasing glyoxal content to 0.3% (A2) and 0.5% (A3) reduced EGCG release. This reduction can be attributed to the enhanced hydrogel network strength at higher crosslinker concentrations, which acts as a barrier to drug diffusion. These findings are consistent with the swelling behavior, where higher glyoxal content decreased the percentage weight increase [35]. Figures 4B and 4D illustrate the effects of chitosan and PVA on EGCG release. Formulation A11, containing low polymer content (1% chitosan and 1% PVA), exhibited the highest EGCG release. Increasing chitosan to 2% (A12) slightly reduced total release to 73%, while higher PVA content (A4–A6) further diminished EGCG release. These results indicate that increasing polymer content enhances the strength of the superporous hydrogel, reduces system elasticity, and acts as a barrier to drug diffusion in simulated gastric fluid (pH 1.2).

The effect of sodium bicarbonate, used as a poring agent, is shown in Fig. 4C. Incorporation of 100 mg and 200 mg of sodium bicarbonate created more pores, promoting EGCG release, whereas 50 mg resulted in lower drug release. Different EGCG loadings (50, 75, and 100 mg) produced similar release profiles, suggesting that drug loading had minimal effect on release under these conditions. As shown in Fig. 4D, PVA content was fixed at 1% to facilitate EGCG release. Among the chitosan-containing formulations (A11–A13), formulation A12 exhibited a more sustained release, achieving nearly 80% release over 8 hours, indicating that chitosan plays a significant role in prolonging drug release from SPHs. In contrast, varying KGM content (1%, 2%, and 3% in A14–A16) resulted in only minor differences in EGCG release, suggesting a less pronounced effect on release kinetics.

#### 3.1.7 Kinetics of drug release

To investigate the release mechanism of EGCG from the SPHs, three formulations were selected: A2 and A12, representing different PVA contents, and A14, representing KGM-containing hydrogels. The *in vitro* release data were fitted to various kinetic models, including zero-order, first-order, Hixson-Crowell, Higuchi, and Korsmeyer-Peppas,

with results summarized in Table 3. The  $R^2$  values for the Higuchi model were higher than those of the other models, particularly for formulation A2, indicating that EGCG release is governed by Fickian diffusion, with the percentage of drug released proportional to the square root of time. Additionally, the release profiles of A12 and A14 fitted the Korsmeyer-Peppas model, with exponent values ( $n$ ) below 0.45, also indicating Fickian diffusion. These results suggest that the dissolution of EGCG, a water-soluble drug, follows Fick's law of diffusion, where the flux from the hydrogel is proportional to the concentration gradient.

**Table 3 Release kinetic constants of EGCG from superporous hydrogels**

Formulations		A2	A12	A14
Zero-order	$r^2$	0.825	0.747	0.696
	$k_0$	15.069	14.360	12.471
First-order	$r^2$	0.923	0.851	0.771
	$k_1$	0.172	0.160	0.127
Hixson-Crowell	$r^2$	0.897	0.878	0.751
	$k_c$	0.296	0.299	0.249
Higuchi	$r^2$	0.985	0.946	0.938
	$k_H$	46.851	48.47	45.107
Korsmeyer-Peppas	$r^2$	0.979	0.985	0.946
	$n$	0.554	0.364	0.375

#### 3.1.8 Determination of drug content

The EGCG content of the superporous hydrogels is summarized in Table 2. The results demonstrated that SPHs can achieve drug loading greater than 85%, with the highest content observed at  $100.86 \pm 4.58\%$ . Increasing the glyoxal content was associated with a lower EGCG loading (A1 > A2 > A3), and similar trends were observed with increasing chitosan (A11 > A12 > A13) and KGM (A14 > A15 > A16) content. This effect can be explained by Khan *et al.* (2014), who reported that higher crosslinker ratios reduce drug release due to stronger physical entanglements between polymers, exerting a greater influence than polymer concentration [36]. Similarly, Neufeld *et al.* (2017) found that higher polymer content in chitosan-based hydrogels slowed drug release because smaller mesh sizes and stronger drug-polymer interactions restrict diffusion [37]. Nevertheless, all formulations met the specified content uniformity limits (85–115%), and the low standard deviations (<5.0%) confirmed uniform drug distribution within the hydrogels.

#### 3.1.9 Erosion behavior of superporous hydrogels

Erosion of superporous hydrogels occurs after full hydration, as the intermolecular forces within the polymer network are insufficient to withstand contraction forces, leading to breakdown into small particles suspended in acidic medium. As shown in Fig. 5A, the lowest glyoxal content (A1) resulted in the greatest erosion, whereas increasing glyoxal to 0.5% (A3) preserved the hydrogel structure, limiting erosion to approximately 11.3% over 48 hours. Chitosan concentration also influenced erosion: formulation A11 (1% chitosan) exhibited 34.5% erosion,

compared with 25.8% for A12 (2% chitosan). Similarly, increasing PVA content in formulations A4–A6 (3–5%) reduced SPH erosion. Figures 5B and 5C show that sodium bicarbonate and EGCG content had minimal effect on erosion, whereas polymer composition played a more significant role. Formulation A12 exhibited approximately 30.9% erosion after 48 hours, higher than formulation A14 (19.6%) despite containing the same PVA and chitosan levels. This suggests that chitosan promotes erosion, while KGM, a high-molecular-weight polymer forming a viscous gel, acts as a protective barrier, reducing surface erosion [38]. Overall, the addition of KGM in formulations A14–A16 strengthened the hydrogel network and decreased erosion.

#### 3.1.10 FT-IR studies

The FT-IR spectrum of formulation A12 (Fig. 6) exhibited a broad band in the 3200–3400  $\text{cm}^{-1}$  region, corresponding to the stretching vibrations of hydroxyl and amine groups involved in strong hydrogen bonding. The noticeable shift of these peaks to lower wavenumbers suggests crosslinking between the hydrogen-containing groups of chitosan and PVA [39]. Peaks observed at 900 and 1125  $\text{cm}^{-1}$ , together with the broad 3000–3600  $\text{cm}^{-1}$  band, confirm the presence of –OH and –NH<sub>2</sub> groups, indicative of polysaccharides such as chitosan in the SPH [40]. Furthermore, no additional peaks were observed in the spectra of chitosan and EGCG, confirming that there is no significant interaction between EGCG and the chitosan polymer.

#### 3.1.11 Morphology

The SEM images of SPHs containing chitosan and PVA are shown in Fig. 7. SEM was performed to characterize the surface and cross-sectional morphology, texture, and porosity of the hydrogels. The images revealed uniform superporous structures with interconnected pores, and no collapse of the SPH framework was observed. These interconnected pores are formed when the monomer solution undergoes effective foaming and foam stabilization, resulting in well-distributed capillary channels that facilitate the penetration of water molecules into the hydrogel network.

### 3.2 In vitro biological activities of EGCG released from films

#### 3.2.1 Antioxidant activity

The antioxidant activity of EGCG powder was evaluated, showing potent activity with an IC<sub>50</sub> value of 2.599 ± 0.139  $\mu\text{g/mL}$ , compared to ascorbic acid as a positive control (IC<sub>50</sub> = 3.180 ± 0.103  $\mu\text{g/mL}$ ). Formulation A12 exhibited an IC<sub>50</sub> of 2.893 ± 0.042  $\mu\text{g/mL}$ , demonstrating that the SPH retained the antioxidant activity of EGCG. These results indicate that the hydrogel structure allows for effective release of EGCG without interfering with its bioactivity.

#### 3.2.2 In vitro cytotoxicity test

The cytotoxicity of EGCG was evaluated on murine macrophage RAW 264.7 cells using the MTT assay, with cell viability expressed as a percentage. Cells were treated for 24 hours with EGCG powder, blank A12, and formulation A12, and compared to indomethacin as a positive control. EGCG, at concentrations of 6.25–100  $\mu\text{g/mL}$  in both powder and formulation A12, showed cell

viability above 80%, indicating no significant cytotoxicity. Based on these results, concentrations within this range were selected for subsequent evaluation of anti-inflammatory activity.

#### 3.2.3 Anti-inflammatory activity

Nitric oxide (NO) production in RAW 264.7 macrophage cells was measured to evaluate the anti-inflammatory effect of EGCG. Inflammation was induced by lipopolysaccharide (LPS), an element of gram-negative bacterial cell walls that stimulates the immune response through TLR-4, leading to a cascade of intracellular signaling and proinflammatory cytokines, for example, TNF- $\alpha$ , IL-1 $\beta$ , and IL-6, [41]. EGCG inhibits inflammation by blocking the stimulation of nuclear factor-kappa B (NF- $\kappa$ B), a transcription factor crucial for inducible nitric oxide synthase (iNOS) expression [42, 43, 44, 45]. In the culture medium, NO levels were determined using the Griess reagent, and anti-inflammatory activity was quantified by the reduction of NO in LPS-stimulated cells. Treatment with formulation A12 at increasing concentrations (6.25 to 100  $\mu\text{g/mL}$ ) resulted in dose-dependent NO inhibition of 11.31 ± 3.56%, 29.90 ± 3.27%, 53.05 ± 5.95%, 73.54 ± 2.79%, and 88.01 ± 1.67%, respectively. The IC<sub>50</sub> value of formulation A12 was 36.52 ± 2.74  $\mu\text{g/mL}$ , comparable to indomethacin (IC<sub>50</sub> = 35.74 ± 1.84  $\mu\text{g/mL}$ ) and slightly higher than EGCG powder (IC<sub>50</sub> = 28.73 ± 1.58  $\mu\text{g/mL}$ ). The slightly reduced efficacy of formulation A12 compared to EGCG powder may be attributed to the weakly basic properties of chitosan, which can affect EGCG stability. Additionally, the modest NO inhibition observed with blank A12 suggests that chitosan itself contributes a minor anti-inflammatory effect.

### CONCLUSIONS

This study successfully developed a gastroretentive superporous hydrogel for the delivery of EGCG, a bioactive compound from green tea, to enhance its gastric retention and protect it from enzymatic metabolism. Poly(vinyl alcohol) was used in combination with chitosan to form the hydrogel, improving water absorption and mechanical strength. The prepared SPHs demonstrated reproducibility using a gas-blowing technique, as confirmed by consistent weight measurements after freeze-drying. Among the tested formulations, the hydrogel containing 2% w/w chitosan and 1% w/w PVA exhibited optimal compressive strength, swelling capacity, and sustained EGCG release, delivering more than 80% of the drug over 8 hours. Importantly, this formulation significantly reduced inflammatory activity by inhibiting NO production in RAW 264.7 macrophages while retaining potent antioxidant activity.

### ACKNOWLEDGEMENTS

The authors would like to acknowledge financial support from the Project of Strengthening Excellence in Pharmacy, Faculty of Pharmaceutical Sciences, Prince of Songkla University

### REFERENCE

1. Tripathi J, Thapa P, Maharjan R, Jeong SH. Current state and future perspectives on gastroretentive drug

- delivery systems. *Pharmaceutics*. 2019;11(4):193. doi: <http://doi.org/10.3390/pharmaceutics11040193>
2. Dai W, Zhang CY, Wang J, Han J, Shao Z, Sun Y. Bioavailability enhancement of EGCG by structural modification and nano-delivery: A review. *J Funct Foods*. 2020;65:103732. doi: <https://doi.org/10.1016/j.jff.2019.103732>
  3. Fang W, Peng ZL, Dai YJ, Wang DL, Huang P, Huang HP. (-)-Epigallocatechin-3-gallate encapsulated realgar nanoparticles exhibit enhanced anticancer therapeutic efficacy against acute promyelocytic leukemia. *Drug Deliv*. 2019;26(1):1058-67. doi: <https://doi.org/10.1080/10717544.2019.1672830>
  4. Eberle VA, Schoelkopf J, Gane PAC, Alles R, Huwyler J, Puchkov M. Floating gastroretentive drug delivery systems: Comparison of experimental and simulated dissolution profiles and floatation behavior. *European Journal of Pharmaceutical Sciences*. 2014;58:34-43. doi: <https://doi.org/https://doi.org/10.1016/j.ejps.2014.03.001>
  5. Vrettos NN, Roberts CJ, Zhu Z. Gastroretentive technologies in tandem with controlled-release strategies: A potent answer to oral drug bioavailability and patient compliance implications. *Pharmaceutics*. 2021;13(10):1591. doi: <https://doi.org/10.3390/pharmaceutics13101591>
  6. Melocchi A, Uboldi M, Inverardi N, et al. Expandable drug delivery system for gastric retention based on shape memory polymers: Development via 4D printing and extrusion. *Int J Pharm*. 2019;571:118700. doi: <https://doi.org/10.1016/j.ijpharm.2019.118700>
  7. Abouelatta SM, Abouelwafa AA, El-Gazayerly ON. Gastroretentive raft liquid delivery system as a new approach to release extension for carrier-mediated drug. *Drug Deliv*. 2018;25(1):1161-74. doi: <https://doi.org/10.1080/10717544.2018.1474969>
  8. Issarachot O, Bunlung S, Kaewkroek K, Wiwattanapatapee R. Superporous hydrogels based on blends of chitosan and polyvinyl alcohol as a carrier for enhanced gastric delivery of resveratrol. *Saudi Pharm J*. 2023;31(3):335-47. doi: <https://doi.org/10.1016/j.jsps.2023.01.001>
  9. Kumari PK, Sharmila M, Yarraguntla SR. Super porous hydrogels: A review. *J Pharm Res Int*. 2020;32:153-65. doi: <https://doi.org/10.9734/jpri/2020/v32i1330595>
  10. Chavda HV, Patel CN. Preparation and in vitro evaluation of a stomach specific drug delivery system based on superporous hydrogel composite. *Indian J Pharm Sci*. 2011;73(1):30-7. doi: <https://doi.org/10.4103/0250-474X.89754>
  11. Triunfo M, Tafi E, Guarnieri A, Salvia R, Scieuzo C, Hahn T, et al. Characterization of chitin and chitosan derived from *Hermetia illucens*, a further step in a circular economy process. *Sci Rep*. 2022;12:6613. doi: <https://doi.org/10.1038/s41598-022-10423-5>
  12. Sahariah P, Gaware VS, Lieder R, Jónsdóttir S, Hjálmsdóttir MÁ, Sigurjonsson OE, et al. The effect of substituent, degree of acetylation and positioning of the cationic charge on the antibacterial activity of quaternary chitosan derivatives. *Mar Drugs*. 2014;12(8):4635-58. doi: <https://doi.org/10.3390/md12084635>
  13. Aranaz I, Alcántara AR, Civera MC, Arias C, Elorza B, Heras Caballero A, et al. Chitosan: An overview of its properties and applications. *Polymers*. 2021;13(19):3256. doi: <https://doi.org/10.3390/polym13193256>
  14. Mandal UK, Chatterjee B, Senjoti FG. Gastroretentive drug delivery systems and their in vivo success: A recent update. *Asian J Pharm Sci*. 2016;11(5):575-84. doi: <https://doi.org/10.1016/j.ajps.2016.04.007>
  15. Mereles D, Hunstein W. Epigallocatechin-3-gallate (EGCG) for clinical trials: more pitfalls than promises? *Int J Mol Sci*. 2011;12(9):5592-603. doi: <https://doi.org/10.3390/ijms12095592>
  16. Chacko SM, Thambi PT, Kuttan R, Nishigaki I. Beneficial effects of green tea: a literature review. *Chin Med*. 2010 Apr 6;5:13. doi: <https://doi.org/10.1186/1749-8546-5-13>
  17. Barik S, Sutar H, Mishra S. Synthesis and characterisation of PVA/PVOH based super porous hydrogel. *J Am Chem Soc*. 2015;10:1-7. doi: <https://doi.org/10.9734/ACSJ/2016/22127>
  18. Sari R, Mulijani S, Suhartini M. Improvement of PVA-glucomanan-acrylamide hydrogel as base material of immobilization. *Jurnal Kimia Valensi*. 2022;8:1-9. doi: <https://doi.org/10.15408/jkv.v8i1.20332>
  19. Laracuenta ML, Yu MH, McHugh KJ. Zero-order drug delivery: State of the art and future prospects. *J Contr Release*. 2020; 327:834-56. doi: <https://doi.org/10.1016/j.jconrel.2020.09.020>
  20. Behera SS, Ray RC. Konjac glucomannan, a promising polysaccharide of *Amorphophallus konjac* K. Koch in health care. *Int J Biol Macromol*. 2016;92:942-56. doi: <https://doi.org/10.1016/j.jbiomac.2016.07.098>
  21. Jahromi LP, Ghazali M, Ashrafi H, Azadi A. A comparison of models for the analysis of the kinetics of drug release from PLGA-based nanoparticles. *Heliyon*. 2020;6(2): e03451. doi: <https://doi.org/10.1016/j.heliyon.2020.e03451>

22. Paul DR. Elaborations on the Higuchi model for drug delivery. *Int J Pharm.* 2011;418(1):13-17. doi: <https://doi.org/10.1016/j.ijpharm.2010.10.037>
23. Zhu W, Long J, Shi M. Release kinetics model fitting of drugs with different structures from viscose fabric. *Materials.* 2023;16(8):3282. doi: <https://doi.org/10.3390/ma16083282>
24. Avachat AM, Kotwal VB. Design and evaluation of matrix-based controlled release tablets of diclofenac sodium and chondroitin sulphate. *AAPS PharmSciTech.* 2007;8(4):51-56. doi: <https://doi.org/10.1208/pt0804088>
25. Vishal Gupta N, Shivakumar HG. Preparation and characterization of superporous hydrogels as gastroretentive drug delivery system for rosiglitazone maleate. *Daru.* 2010;18(3):200-10. doi: <https://doi.org/10.1080/00914037.2012.735297>
26. Chavda HV, Patel CN, Karen HD. Preparation and characterization of chitosan-based superporous hydrogel composite. *J Young Pharm.* 2009;1:199-204. doi: <https://doi.org/10.4103/0975-1483.57064>
27. Lei J, Gao Y, Xu S, He L, Liu Z. The effect of the effective polymer network on the extremely large deformation and fracture behaviors of polyacrylamide hydrogels. *J Mech Phys Solids.* 2025;200: 106124. doi: <https://doi.org/10.1016/j.jmps.2025.106124>
28. Bui N, Nguyen G, Nguyen, A, Nguyen T. Crosslinked hydrogel based on Polyvinyl alcohol/chitosan/glyoxal for the removal of Crom(VI) ions from aqueous solution. *STDJ.* 2024;6:63-72. doi: <https://doi.org/10.32508/stdjet.v6iSI3.1239>
29. Chavda H, Modhia I, Mehta A, Patel R, Patel C. Development of bioadhesive chitosan superporous hydrogel composite particles based intestinal drug delivery system. *Biomed Res Int.* 2013;2013:563651. doi: <https://doi.org/10.1155/2013/563651>
30. Cen C, Wang F, Wang Y, et al. Design and characterization of an antibacterial film composited by hydroxyethyl cellulose (HEC), carboxymethyl chitosan (CMCS), and nano ZnO for food packaging. *Int J Biol Macromol.* 2023;231:123203. doi: <https://doi.org/10.1016/j.ijbiomac.2023.123203>
31. Sun Y, Xu X, Zhang Q, Zhang D, Xie X, Zhou H, Wu Z, Liu R, Pang J. Review of Konjac Glucomannan Structure, Properties, Gelation Mechanism, and Application in Medical Biology. *Polymers.* 2023; 15(8):1852. doi: <https://doi.org/10.3390/polym15081852>
32. Yui T, Ogawa K, Sarko A. Molecular and crystal structure of konjac glucomannan in the mannan II polymorphic form. *Carbohydr Res.* 1992;229(1):41-55 doi: [https://doi.org/10.1016/s0008-6215\(00\)90479-8](https://doi.org/10.1016/s0008-6215(00)90479-8)
33. Ghazali S, Adnan N. Effect of foaming agent on the properties of superporous hydrogels prepared via solution polymerization method. *Indian J Sci Technol.* 2017;10(6):1-6. doi: <https://doi.org/10.17485/ijst/2017/v10i6/111214>
34. Ding P, Sun Y, Jiang G, Nie L. Hydroxyproline-modified chitosan-based hydrogel dressing incorporated with epigallocatechin-3-gallate promotes wound healing through immunomodulation. *Gels.* 2025;11(9):732. doi: <https://doi.org/10.3390/gels11090732>
35. Nasution H, Harahap H, Dalimunthe NF, Ginting MHS, Jaafar M, Tan OOH, et al. Hydrogel and effects of crosslinking agent on cellulose-based hydrogels: A review. *Gels.* 2022; 8(9):568. doi: <https://doi.org/10.3390/gels8090568>
36. Khan S, Ranjha NM. Effect of degree of cross-linking on swelling and on drug release of low viscous chitosan/poly(vinyl alcohol) hydrogels. *Polymer Bulletin.* 2014;71(8): 2133-58. doi: <https://doi.org/10.1007/s00289-014-1178-2>
37. Neufeld L, Bianco-Peled H. Pectin–chitosan physical hydrogels as potential drug delivery vehicles. *Int J Biol Macromol.* 2017;101:852-861. doi: <https://doi.org/10.1016/j.ijbiomac.2017.03.167>
38. Haruna MH, Wang Y, Pang J. Konjac glucomannan-based composite films fabricated in the presence of carnauba wax emulsion: hydrophobicity, mechanical and microstructural properties evaluation. *J Food Sci Technol.* 2019;56(11):5138-5145. doi: <https://doi.org/10.1007/s13197-019-03932-1>
39. Abureesh MA, Oladipo AA, Gazi M. Facile synthesis of glucose-sensitive chitosan-poly(vinyl alcohol) hydrogel: Drug release optimization and swelling properties. *Int J Biol Macromol.* 2016;90:75-80. doi: <https://doi.org/10.1016/j.ijbiomac.2015.10.001>
40. Acik G. Soybean oil modified bio-based poly(vinyl alcohol)s via ring-opening polymerization. *J Polym Environ.* 2019;27:2618–23. doi: <https://doi.org/10.1007/s10924-019-01547-3>
41. Arya P, Sharma V, Singh P, Thapliyal S, Sharma M. Bacterial endotoxin-lipopolysaccharide role in inflammatory diseases: An overview. *Iran J Basic Med Sci.* 2025;28(5): 553–64. doi: <https://doi.org/10.22038/ijbms.2025.82302.17799>
42. Kim SR, Seong KJ, Kim WJ, Jung JY. Epigallocatechin gallate protects against hypoxia-induced inflammation in microglia via NF-κB suppression and Nrf-2/HO-1 activation. *Int J Mol Sci.* 2022; 23(7):4004. doi: <https://doi.org/10.3390/ijms23074004>
43. Ghuriani, V., Wassan, J. T., Deolal, P., Sharma, V., Dalal, D., & Goyal, A. (2023). An integrative approach towards recommending farming solutions for sustainable agriculture. *Journal of Experimental Biology and Agricultural Sciences,* 11(2), 306–315. doi: [https://doi.org/10.18006/2023.11\(2\).306.315](https://doi.org/10.18006/2023.11(2).306.315)
44. Al-Sharqi, A. A., Dari, W. A., Jassim, R., Mohsin, Y. B., Hussian, A. K., & Mohmood, R. R. (2025). The synergistic effects of *Lactobacillus acidophilus* and

*Chlorella* spp. against pathogens isolated from dermal infections. *International Journal of Probiotics and Prebiotics*, 20, 19–23. <https://doi.org/10.37290/ijpp2641-7197.20:19-23>

45. Alshahrani, S. M. (2024). Knowledge, attitudes, and barriers toward using complementary and alternative

medicine among medical and nonmedical university students: A cross-sectional study from Saudi Arabia. *Current Topics in Nutraceutical Research*, 22(3), 889–894. <https://doi.org/10.37290/ctnr2641-452X.22:889-894>